

3.6.5

Development and future prospects of wavelength shifting fibre detectors at ISIS

G. Jeff Sykora¹, Erik M. Schooneveld¹ and Nigel J. Rhodes¹

¹Instrumentation Division, STFC, ISIS Facility, Rutherford Appleton Laboratory, Harwell Oxford, United Kingdom

E-mail: Jeff.sykora@stfc.ac.uk

Abstract. Recent advances in WLSF detector technology at ISIS are presented here. Cost reduction strategies, such as a transition from single anode to multi-anode PMTs and optically isolated scintillator elements to continuous scintillator sheets, will be discussed. Advantages and current disadvantages of WLSF detector technology will also be discussed. Thermal neutron detection efficiencies of approximately 65% with corresponding gamma sensitivities on the order of 10^{-7} are shown. Pixel to pixel variation of less than $\pm 6\%$ has been achieved for linear and 2D position sensitive detectors. These properties make WLSF detectors viable for a variety of applications at ISIS.

1. Introduction

Scintillation detectors using ZnS:Ag/⁶LiF are currently used in a number of facilities such as J-PARC [1], [2], SNS [3] and ISIS. At the ISIS pulsed neutron and muon scattering facility, these scintillation detectors have been employed for more than two decades and service approximately half of the instruments [4]. The current generation of ZnS:Ag/⁶LiF detectors on ISIS are optically coupled to photomultiplier tubes (PMT) with clear optical fibres [4]. New instruments will, however, require larger area or finer resolution detectors which render clear optical fibres obsolete due to high costs and manufacturing difficulties. J-PARC and SNS have ZnS:Ag/⁶LiF detectors operational that are using wavelength shifting fibre (WLSF) instead of clear optical fibres and are considerably cheaper to produce with reduced manufacturing complications. ISIS is therefore also developing WLSF based ZnS:Ag/⁶LiF detectors.

ISIS, along with other facilities, is developing WLSF detector technology to suit a variety of instruments. IMAT is the first ISIS instrument planning on using WLSF detectors on a large scale [5]. Modifications to the IMAT detector design have made WLSF detectors useful for a broad range of neutron scattering applications including current reflectometers and future single crystal diffractometers.

Details of neutron scattering applications at ISIS suitable to WLSF detector technology are described below. Developments in WLSF detector technology for a broad range of applications are discussed in terms of instrument specifications.

2. Detector requirements for new and upgraded instruments

ZnS:Ag/⁶LiF scintillator detectors on ISIS have generally serviced low rate (<5 kHz local peak rate) powder diffractometers, like ENGIN-X, POLARIS, GEM, HRPD and PEARL. Some of these powder diffractometers will soon be due for upgrades which will include larger area coverage. Reflectometers

like CRISP and SURF on TS1 operate with clear fibre coupled scintillator limiting the position resolution of the detector to 1.2mm and are thus due for upgraded detectors.

New instruments like IMAT, which is currently under construction, and LMX, which is proposed for a future phase of TS2, are good candidates for WLSF detectors because of their unique requirements. Future prospects of WLSF detectors on ISIS also include large inelastic spectrometers. These spectrometers are usually equipped with ^3He detectors, but ^3He has become rare and expensive [6], [7]. Instruments suited to WLSF detectors and their detector requirements are described below.

2.1 IMAT

IMAT is an imaging and diffraction instrument for materials science utilizing a new technique called tomography driven diffraction [8]. The diffraction detector suite will include the ability for strain and texture analysis. In order for the instrument to operate efficiently, there must be high angular coverage with detector pixilation for texture analysis. Diffraction banks are proposed to cover a total of 18m^2 with detector banks at 2theta positions of 20, 45, 90, 125 and 155 degrees. The secondary flight path of the 90 degree bank will be 2 m [5]. The detector array will require 2 dimensional positioning to facilitate texture analysis. Each detector will consist of pixels $4\text{mm} \times 100\text{mm}$ with minimal dead space to provide d-spacing resolution $\Delta d/d = 0.7\%$ at 90 degrees. The detector will need to cope with approximately 10 kHz local peak rate.

2.2 Linear reflectometers – CRISP

CRISP was the first neutron reflectometer on ISIS and is designed to study interfacial phenomena with the ability to perform polarized neutron reflectometry [9], [10]. Currently, a clear optical fibre coded ZnS:Ag detector with 260mm linear coverage is used to detect off-specular reflections. Clear optical fibre coupling limits the position resolution of the detector to 1.2mm and is reported to limit the rate capability of the instrument. Future experiments will likely require 0.5mm linear position resolution with a factor of 10 improvement in the current count rate capability of 1.5kHz per detector pixel. Off-specular reflectivity also requires elimination of ghosting artefacts which exist in the current detector.

2.3 2D reflectometers – Surf, Inter, PolRef and OffSpec

The current suite of reflectometers is operated with linear position sensitive detectors (PolRef, OffSpec and Inter) similar to that on CRISP described above. Surf utilizes a small 2D clear fibre coupled ZnS:Ag/ ^6LiF detector [11]. In some cases, users need to have horizontal as well as vertical position sensitivity which requires rotation of the detector by 90 degrees and a second data set. 2D detectors would greatly simplify the process as well as add to the scientific merit of some experiments. The 2D detectors would be required to maintain similar 1.2mm position resolution. As with a linear reflectometer detector, count rate improvements of over a factor of 10 are desired while maintaining a high degree of pixel to pixel uniformity.

2.4 LMX

LMX is a proposed high flux single crystal diffractometer which will be used for large molecular crystallography [12]. Single crystal diffraction requires 2 dimensional detectors. Small proposed secondary flight paths between 0.25m – 0.75m require the detector to have a maximum position resolution of $1\text{mm} \times 1\text{mm}$ ($0.5\text{mm} \times 0.5\text{mm}$ is preferable) and be insensitive to parallax errors.

2.5 Inelastic spectrometers

Current inelastic neutron spectrometers like LET on TS-2 cover large areas (up to 40m^2) and use resistive wire ^3He tubes [13]. Due to very limited supply of ^3He , the amount of ^3He required for such detectors is now too large to be considered in future inelastic spectrometers. Detector requirements for future inelastic spectrometers would be similar to LET, i.e. a coarse 2 dimensional position resolution

(20mm x 20mm) with neutron detection efficiency better than 80% at 1.8Å, low intrinsic background and insensitivity to gamma (around 10^{-7}).

3. Wavelength shifting fibre detector variations

Wavelength shifting fibre coupled ZnS:Ag/⁶LiF detectors offer significant advantages in cost savings, ease of assembly and are ideally suited to provide fine position resolution requirements. Development has been focused on maintaining high detection efficiencies and reliability. These detectors are described below.

3.1 Linear Position Sensitive Detectors – Diffractometers and reflectometers

Two styles of linear WLSF detectors have been developed, one has complete optical isolation (called the isolated linear detector) and another is a low-cost solution without optical isolation (called the continuous linear detector). Photographs of the two detector types are shown in Figure 1. The isolated linear detector was developed as a solution to general powder diffractometers with the guarantee of complete optical isolation in the scintillator-fibre head. Constraining the light to a single detector pixel prevents misplacement of neutron events (known as ghosts) and multi-counts due to light spread across the detector.

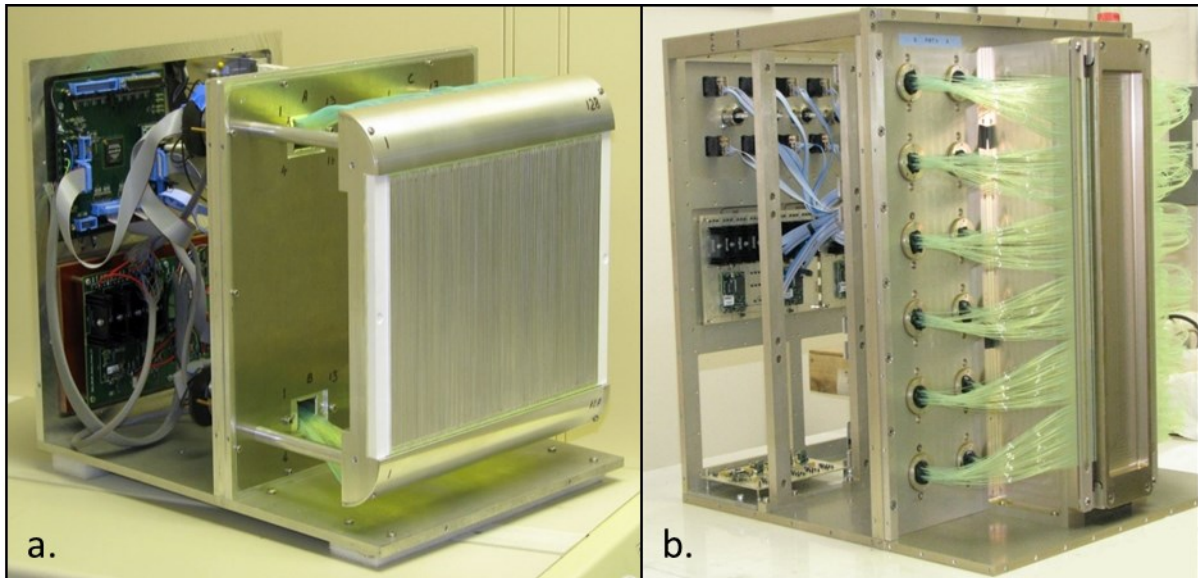


Figure 1. Photographs of the isolated linear detector (a.) and the continuous linear detector (b.).

The isolated linear detector was constructed with 2 mm wide and 200 mm long pixels. Each pixel consisted of two 1mm diameter wavelength shifting fibres sandwiched between two 0.46 mm thick ZnS:Ag/⁶LiF scintillator (AST [14] 2:1 scintillator) strips and wrapped in thin aluminium foil. Two scintillator strips were used to increase neutron absorption efficiency compared to a single sheet. A dual coincidence fibre code was used to eliminate PMT noise events and decrease the number of PMTs used to read out the detector. The fibres were coded such that four scintillator elements were viewed by a single pixel of a Hamamatsu H8711 16 channel multi-anode PMT (MA-PMT). A Photograph of the detector is shown in figure 1a. Figure 2 shows the neutron detection efficiency of the isolated linear detector as a function of wavelength compared to that of a 6 bar ³He detector measured at Reactor Institute Delft (RID). The isolated linear detector was 65% efficient at 1.8Å, has 2mm position resolution, 16 kHz maximum local count rate capability and 3×10^{-7} gamma sensitivity. A detailed study of the isolated linear detector at RID can be found elsewhere [15].

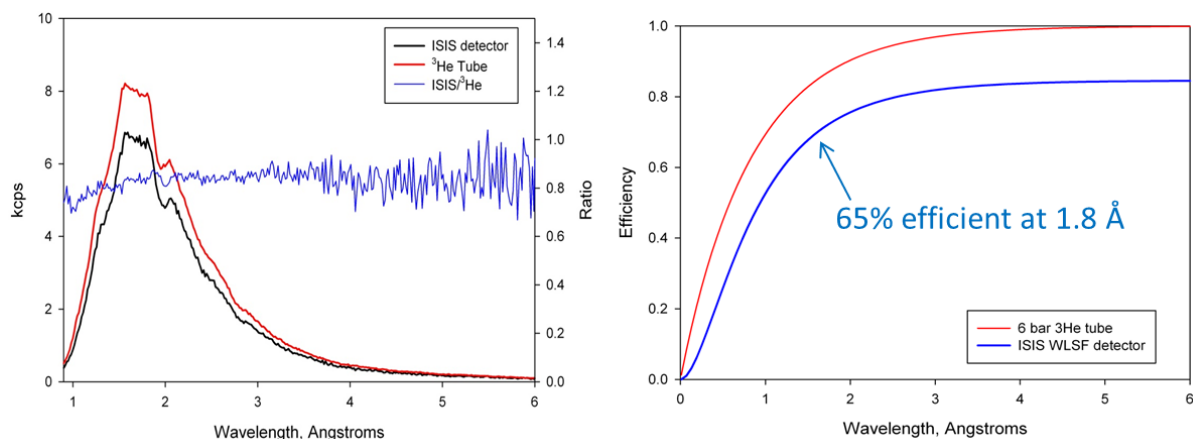


Figure 2. (Left) Time-of-flight neutron spectra as detected by a 6 bar, 25.4mm ³He tube (red line) and isolated linear detector (black line) and the ratio between the two (blue line). (Right) Calculated efficiency as a function of wavelength for the ³He tube and the isolated linear detector.

An isolated detector is relatively difficult to assemble due to cutting the scintillator and wrapping individual scintillator elements. It is also practically impossible to build a detector with less than 2mm position resolution with the optically isolated pixel concept. Constructing a detector with single, continuous, sheets of ZnS:Ag/⁶LiF solves these issues.

The continuous linear detector (pictured in figure 1b) was constructed to suit the CRISP reflectometer needs. The detector consisted of parallel rows of 768 fibres that were 0.5mm in diameter. The fibres were sandwiched between two single sheets of 406mm x 66mm x 0.46mm AST 2:1 scintillator which were placed so their inside surfaces were in contact with the fibres. Fibres were coded into 24, 16-channel, MA-PMTs. Every other pixel of the PMT was used (called the active PMT pixel) to eliminate cross-talk between PMT channels. Each active PMT pixel was coupled to one end of 8 fibres. A dual coincidence fibre code was optimized to minimize the possibility of ghosting and optimize global count rate capability.

Ghosting occurs as a result of scintillation light from one neutron overlapping in time with afterglow of another neutron interacting in a different location in the detector. Despite limiting ghosting with the chosen fibre code, light spread in the scintillator-fibre head increases the chances of ghosting. A signal processing algorithm was developed to eliminate ghosting artefacts. The algorithm resulted in at least a factor of 10 reduction in ghosts with only a 15% decrease in neutron detection efficiency (from 65% to 56% at 1.8Å). Details of the ghost reduction algorithm are beyond the scope of this paper. Position resolution was determined to be 0.7mm which is considerably better than the 1.2mm position resolution of the detectors used on CRISP. It is believed that light spread coupled with a simple position determination algorithm broadens the peaks beyond the fibre pitch.

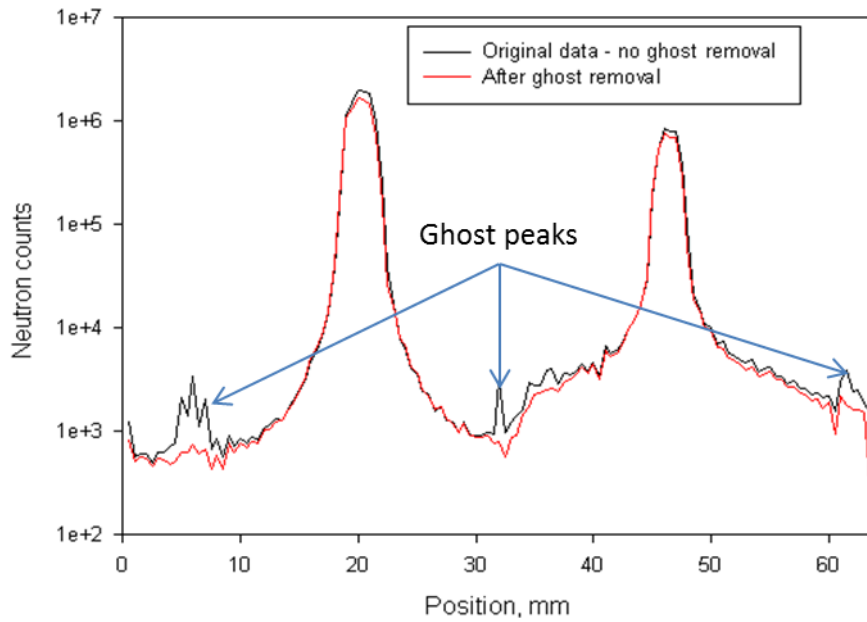


Figure 3. Position spectrum of the continuous linear detector measured on the CRISP beamline with a super mirror sample depicting results of the ghost removal processing algorithm.

3.2 IMAT detector options

IMAT requires 4mm resolution in 2θ and coarse 100mm resolution in the azimuthal direction. Rectangular pixel sizes needed for IMAT led to three possible geometries as shown in Figure 4. In the first geometry, WLS fibres were divided by reflective slats defining the pixel dimensions to be 4mm x 100mm. Reflective slats were used to prevent excessive light spread. Two continuous sheets of 0.46mm thick AST 2:1 scintillator were fixed in contact with the slats. A small amount of scintillation light is still able to spread into the adjacent pixel because of light scattering in the scintillator (called scintillator cross-talk). This effect was minor and was eliminated by a cross-talk reduction algorithm in the electronics. In this solution, the fibres were sharply bent at 2.5mm radius to allow stacking in the (coarse) azimuthal direction with minimum dead space. Two fibres were spaced evenly in each detector pixel to decrease the number of fibres and therefore decrease the amount of labour needed to produce the detector. Spacing of the fibres resulted in less light collection but maintained overall neutron detection efficiency at the operating discriminator level (200mV). The black curve in figure 5 shows the normalized count-rate of this solution as a function of discrimination level.

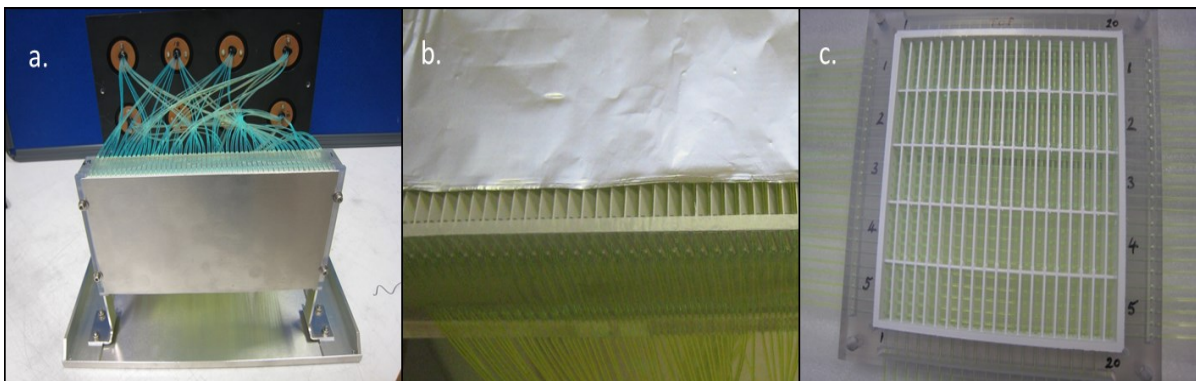


Figure 4. Photographs of the IMAT detector options. (a.) Is a continuous flat scintillator sheet with 2.5mm bend radius fibres, (b.) is a zoomed in photo of the venetian scintillators and (c.) is the fibre support grid for the crossed-fibre detector.

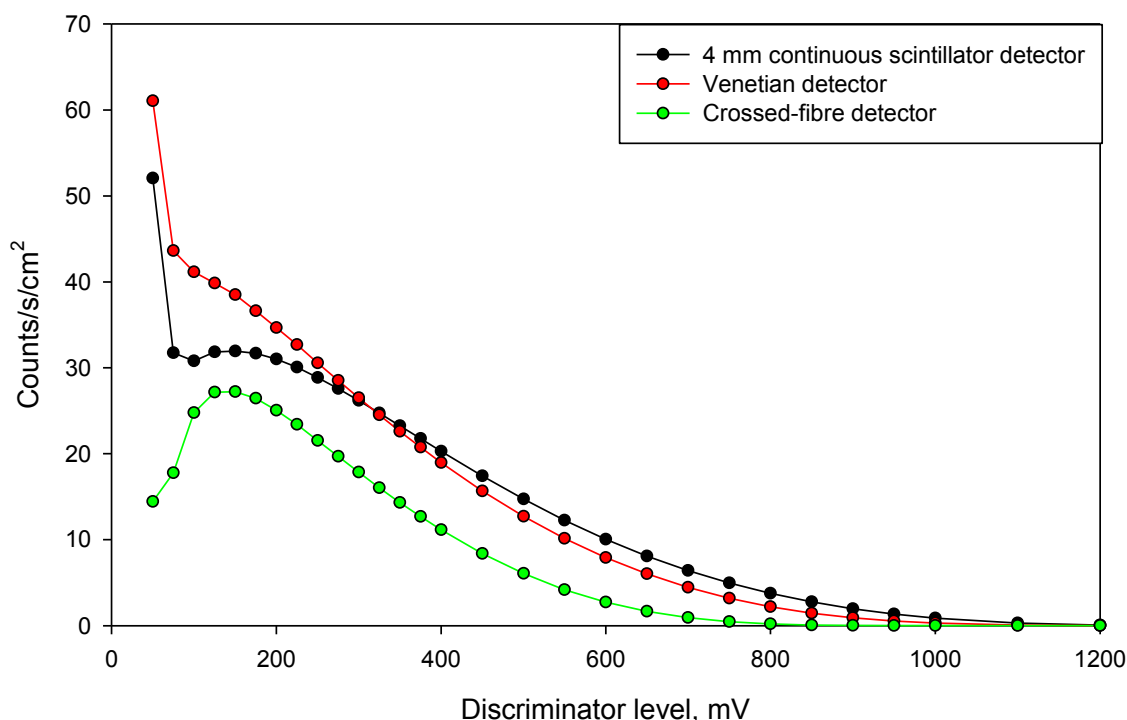


Figure 5. Plot of the area and time normalized counts as a function of discriminator level for the three IMAT detector options, measured with a $^{241}\text{AmBe}$ source. This plot shows the relative efficiencies and light collection of each detector.

The second solution (pictured in Figure 4b) again used a linear array of sharply bent fibres but has scintillators that are individually cut and angled at 72 degrees relative to the neutron’s angle of incidence (called a Venetian geometry). The Venetian geometry was chosen to increase the neutron absorption efficiency by virtue of longer path lengths of the neutron through the scintillator. Each scintillator had a reflector attached to the back of it and the entire active area was covered in Aluminium foil to prevent light spread into adjacent detector pixels. The overall pixel size was 4mm x 100mm. The fibres were coded into 38mm single anode PMTs. As in the continuous scintillator detector, the linear detectors are stacked to provide azimuthal position sensitivity.

Figure 6 is a plot of the efficiency as a function of wavelength for the Venetian geometry relative to the flat geometry detector. There is a 15% increase in efficiency at 1.8\AA which is attributed to the increased path length in the scintillator. There is as much as a 40% increase in efficiency at long wavelengths which is a result of the ability of light to escape the scintillator and efficiently collected by the fibres. Long wavelength neutrons are absorbed at the surface of the scintillator resulting in scintillation occurring at the surface. In the flat geometry, scintillation light is scattered through the bulk of the opaque scintillator. These events have the least amount of light collected and are the most difficult to detect. In the Venetian geometry, low energy neutrons are absorbed at the surface nearest the fibres making those events the brightest and thus easiest to detect.

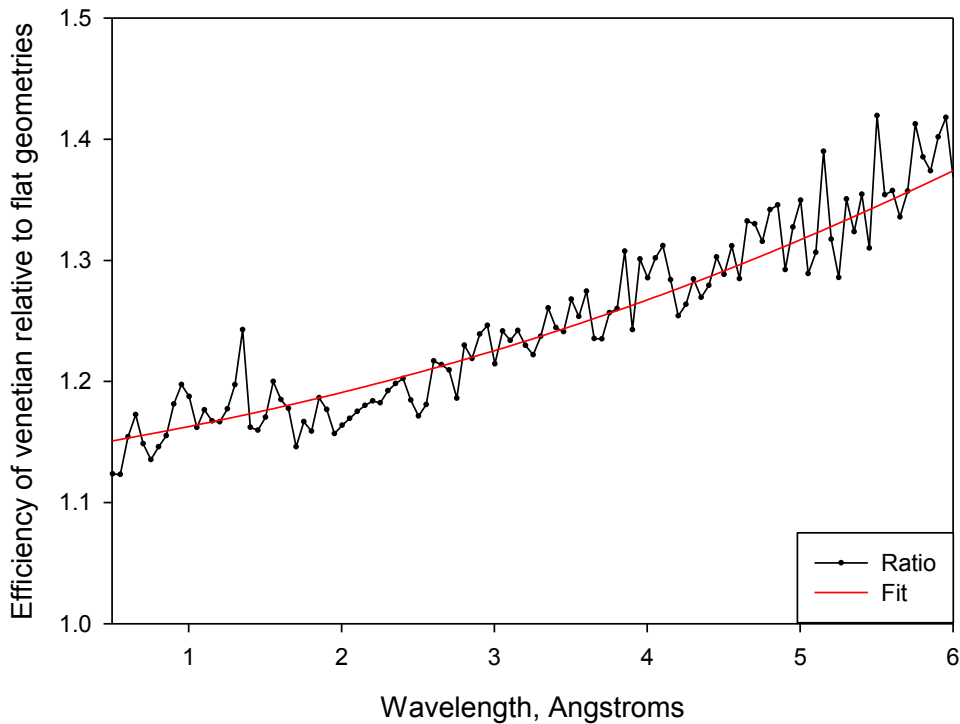


Figure 6. Relative efficiency of the Venetian geometry compared to the continuous flat scintillator detector option for IMAT.

The third solution is a 2-dimensional crossed fibre detector pictured in Figure 4c. The 2theta plane is coded into 4mm pixels and the azimuthal direction is coarsely coded into 20mm pixels making a single pixel 4mm x 20mm. The crossed-fibre support was constructed such that each detector pixel was optically isolated by a thin wall coated with reflective paint. Two continuous sheets of 0.46mm thick AST 2:1 scintillator were placed on the top and bottom of the fibre support. Fibres were coded into 16-channel MA-PMTs. Different pixel sizes can be obtained by either different fibre coding or re-binning the data to make larger pixels. 4-fold fibre coding coincidence was used in order to reduce the number of PMTs needed.

As seen in Figure 5, the crossed-fibre approach suffers from reduced efficiency due to 4 fold coincidence. Efficiency is reduced by approximately 30%. This reduction in efficiency is likely a convolution of effects from the 4-fold coincidence and optical cross-talk in the MA-PMTs. When the PMTs in each plane of fibres were summed to simulate 2-fold coincidence, the efficiency is the same as isolated linear detector (or approximately 65% at 1.8Å). This demonstrates that neutrons are being absorbed, but not detected with 4-fold coincidence.

3.3 2D fine resolution – reflectometers and LMX

A unique 3-layer crossed-fibre detector (pictured in figure 7) was developed as a solution to suit the needs of single crystal diffractometers and reflectometers. 1mm diameter WLS fibres were placed on a 1mm pitch. Top and bottom layers contained 60ppm of dye allowing partial transmission of light to the middle layer. The middle layer was highly absorbing, with a dye content of 300ppm. Top and bottom layers were read out separately and provide horizontal position information while the middle layer provides vertical position information. 3 fibre layers allowed for scintillators to be placed on both the top and bottom of the fibre support system while helping to reduce light spread in the scintillator-fibre cavity.

Fibre ends were coded in 4-fold coincidence into six 16 channel MA-PMTs. 4-fold coincidence coding allowed for 16384 pixels (128x128 pixels) to be readout by 96 PMT channels with 8 fibre ends coupled to each PMT pixel. In the first instance, only one quadrant of the detector could be read out due to limitations on the number of available electronics channels. No fundamental problems prevent readout of the entire detector.

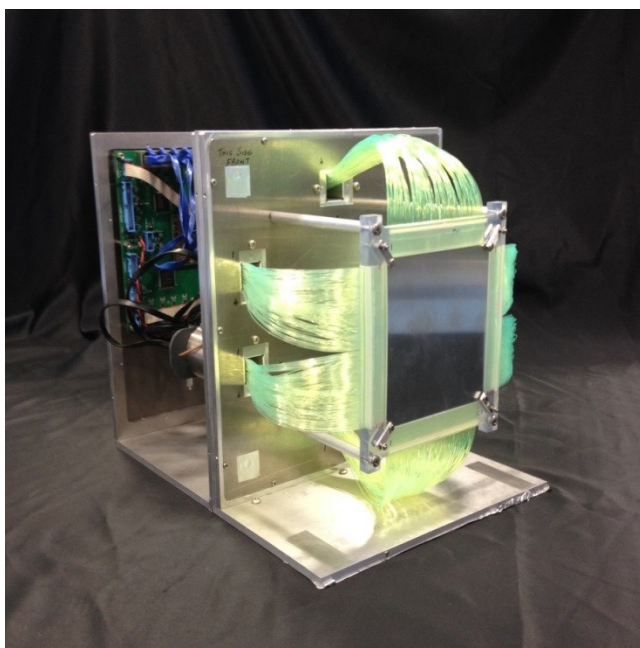


Figure 7. Photograph of the 2D fine resolution detector concept.

4-fold coincidence coding reduced the efficiency of the detector from the nominal 65% at 1.8Å to approximately 40%, as in the IMAT crossed-fibre detector. Light spread from the scintillator to the second layer of fibres also complicates positioning algorithms causing events to be rejected. Signal processing and position reconstruction algorithms are currently under development to improve event recognition and increase efficiency.

An image of the position reconstruction of a Cd mask as well as the position resolution are shown in Figure 8. Full-width at half maximum gives the position resolution to be 1.2mm. Light spread in the scintillator likely causes a small ambiguity in positioning causing slight broadening beyond the 1mm fibre pitch. 1.2 mm spatial resolution is sufficient for an instrument like LMX. Resolution could be further improved by using smaller diameter fibres and more sophisticated positioning algorithms.

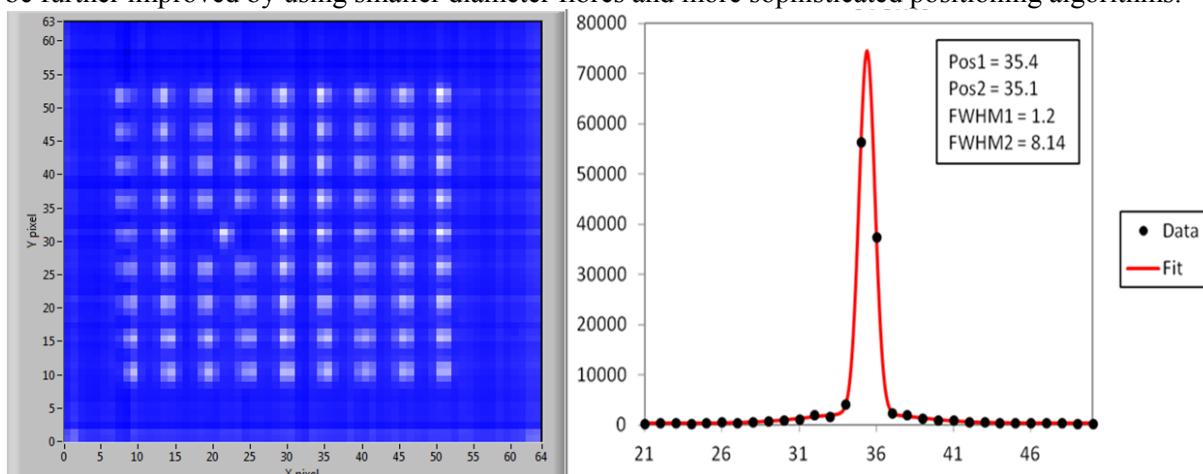


Figure 8. (Left) 2D position reconstruction of a Cd mask on top of the detector and (right) Gaussian fit of the counts in the middle layer of the detector behind a mask of 0.7mm diameter showing position resolution of 1.2mm.

3.4 2D coarse resolution – inelastic spectrometers

A coarse 2D detector, shown in Figure 9, was built with pixel sizes similar to that of resistive wire ³He tubes. An optically isolating, plastic fibre support grid was printed with 20mm x 20mm pixels arranged in an 8x8 array (160mm x 160mm overall active area). The fibre grid had guide holes on a

5mm pitch. The WLS fibres were placed in the grid in orthogonal planes to provide 2D position information. Two continuous sheets of 0.46mm thick 2:1 AST ZnS:Ag/⁶LiF scintillators on aluminium backing plates were placed directly on the grid facing the fibres. Fibres in each row and column of detector pixels were coupled to separate pixels on a MA-PMT providing a 2 fold coincidence for every detector pixel. 64 pixels were read out by a single 16 channel MA-PMT.

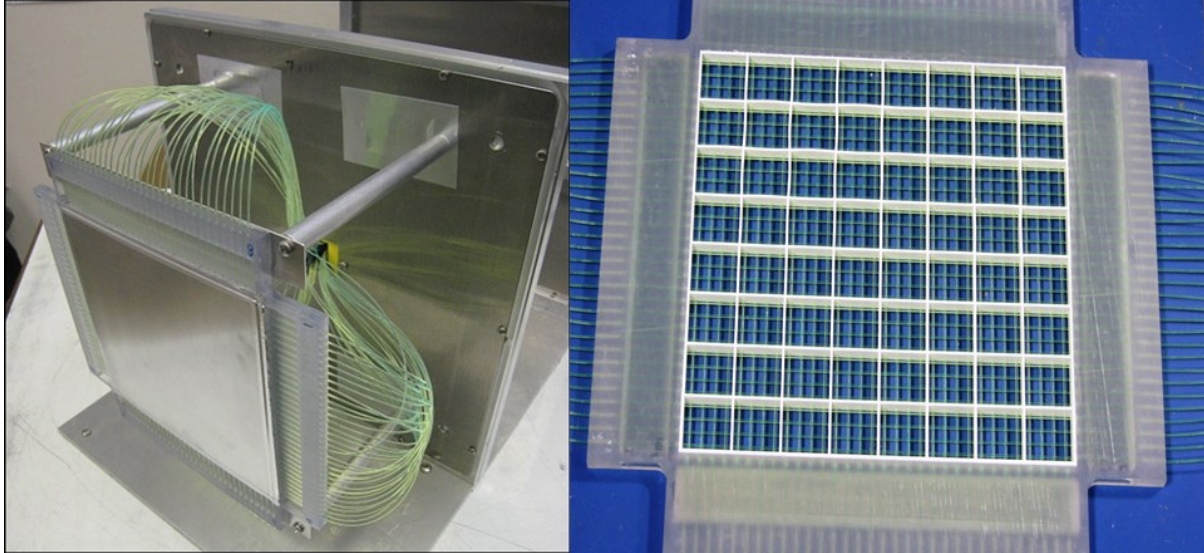


Figure 9. Photographs of the 2D coarse resolution concept and fibre support grid.

Neutron detection efficiency of the 2-fold coarse resolution 2D detector was 65% at 1.8Å, the same as the theoretically expected detection efficiency, despite having a large fibre pitch. Figure 10 shows the efficiency and light collection of the coarse 2D detector relative to the isolated linear detector. Light collection is lower than the isolated linear detector due to the large fibre pitch. Reduced counts for the detector with a standard position reconstruction algorithm (black curve) at low discriminator values are a result of light cross-talk, mainly on the MA-PMT. The red curve in figure 10 demonstrates that light cross-talk is eliminated by a cross-talk reduction algorithm in signal processing.

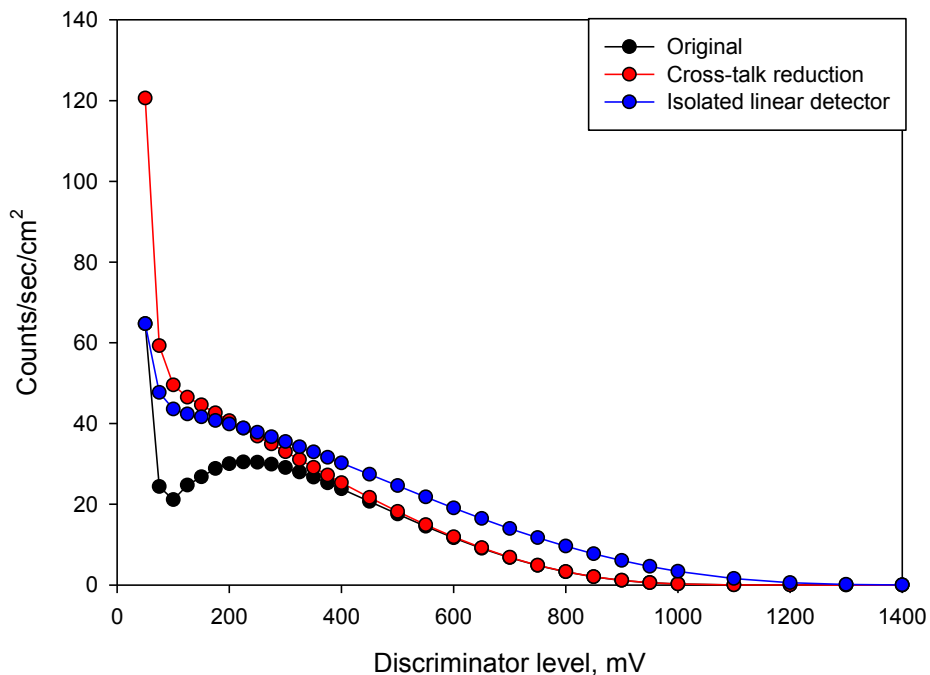


Figure 10. Plot of the area and time normalised counts as a function of discriminator level for the coarse 2D detector showing light collection and efficiency compared to the isolated linear detector measured with a ²⁴¹AmBe source.

One problem with the current coarse 2D detector is the inherent sensitivity to background radiation. Currently, ^3He detectors have background count rates of approximately 0.1 counts per hour per cm^2 , whereas the (2-fold coincidence) scintillator detector is approximately a factor of 30 worse than that. In general, 4-fold coincidence detectors have a lower background rate than 2-fold coincidence detectors. The sensitivity to background radiation of the coarse 2D detector therefore might be improved by using a 4-fold coincidence read out, provided that acceptable detection efficiency can be achieved.

4. Conclusions

Current WLSF detectors have shown exceptional performance in terms of efficiency, position resolution and gamma sensitivity. There are now WLSF detector options for general powder diffraction, the IMAT 90 degree bank, 1D and 2D reflectometry, single crystal diffraction and inelastic spectroscopy. There are still challenges to overcome in order to take full advantage of some instruments. Reflectometers could be more effective if the rate capability of the detectors was increased. The background of WLSF detectors needs to be reduced for inelastic spectroscopy. Research and development is ongoing to address these issues. Despite these challenges, wavelength shifting fibre detector technology is versatile and ideally suited to many applications.

5. Acknowledgements

The authors would like to thank the ISIS neutron detector group for their support, particularly Brian Holland for his invaluable contribution to detector assembly. A portion of the ^3He replacement detector work was funded by the NMI3-II Grant Agreement no. 283883.

Appendix A. Evaluation procedures

All detectors undergo the same initial evaluation procedure to ascertain relative thermal neutron detection efficiency, pixel to pixel uniformity and light collection capability. After initial evaluation has been performed, detector requirement specific tests are performed on a beam line at ISIS. Beam line tests are performed to verify position resolution, rate capability, ghosting, wavelength dependent neutron detection efficiency and uniformity.

Initial evaluations are performed by irradiating the detector with neutrons from a water moderated $^{241}\text{AmBe}$ source. Moderated $^{241}\text{AmBe}$ is a broad spectrum neutron source with median energy at 25meV and a significant, but undetermined, contribution of fast neutrons. Every detector was placed approximately 30cm from the face of the moderator such that the main flux was perpendicular to the face of the detector. It has been established that at this position, using a 200mV discrimination level, a count-rate of 40 counts/sec/ cm^2 for a detector with two continuous sheets of 0.46mm thick 2:1 AST ZnS:Ag/ ^6LiF scintillators corresponds to a detection efficiency of 65% for 1.8Å neutrons.

The ALF and CRISP instruments on ISIS were used to evaluate wavelength dependent efficiency, position resolution, rate capability and ghosting. EMMA is a new instrument on ISIS and was used to investigate positioning accuracy of the detector. ALF is a general purpose TOF instrument used for crystal alignment and detector testing. ALF views the 95K methane moderator and has a wavelength range of 0.6Å – 5.2 Å. Detectors can be placed either in the beam or in scattering. The CRISP TOF reflectometer [9], [10] was operated in un-polarized mode with a wavelength range of 0.5Å to 12Å with the T-Zero chopper running at 25 Hz. Beam slits on CRISP allowed for easy control of the beam size and flux on the detector. EMMA is the new equipment, materials and mechanics analyzer built in place of the previously decommissioned HET chopper spectrometer. EMMA has a dedicated detector testing blockhouse with the option of operating as a chopper spectrometer. EMMA views the room temperature water moderator providing wavelength range from 0.2Å to 3Å.

All detectors were purpose built to address different needs and as such were subject to different test conditions. Specific test conditions were not described in detail because more details will be elaborated on in future publications.

References

- [1] Y. Ikeda 2009, "J-PARC status update," *Nucl. Instr. Meth. Phys. Res. A*, **600**, 1-4
- [2] T. Nakamura, T. Kawasaki, T. Hosoya, K. Toh, K. Oikawa, K. Sakasai, M. Ebine, A. Birumachi, K. Soyama and M. Katagiri 2012, "A large-area two-dimensional scintillator detector with a wavelength-shifting fibre readout for a time-of-flight single-crystal neutron diffractometer," *Nucl. Instr. Meth. Phys. Res. A*, **686**, 64-70
- [3] M. L. Crow, J. P. Hodges and R. F. Cooper 2004, "Shifting scintillator prototype large pixel wavelength-shifting fiber detector for the POWGEN3 powder diffractometer," *Nucl. Instr. Meth. Phys. Res. A*, **529**, 287-292
- [4] N. J. Rhodes, E. M. Schooneveld and R. S. Eccleston 2004, "Current status and future directions of position sensitive neutron detectors at ISIS," *Nucl. Instr. Meth. Phys. Res. A*, **529**, 243-248
- [5] W. Kockelmann, S. Zhang, J. Kelleher, J. Nightingale, G. Burca and J. James 2013, "IMAT – a new imaging and diffraction instrument at ISIS," *Physics Procedia*, **43**, 100-110
- [6] D. A. Shea and D. Morgan 2010, "The Helium-3 Shortage: Supply, Demand and Options for Congress," CRS Report for Congress
- [7] R. T. Kouzes, A. T. Lintereur and E. R. Siciliano 2014, "Progress in alternative neutron detection to address the helium-3 shortage," *Nucl. Instr. Meth. Phys. Res. A*, **784**, 172-175
- [8] G. Burca, J. James, W. Kockelmann, M. Fitzpatrick, S. Zhang, J. Hovind and R. van Langh 2011 "A new bridge technique for neutron tomography and diffraction measurements," *Nucl. Instr. Meth. Phys. Res. A*, **651**, 229-235
- [9] J. Penfold, R. C. Ward and W. G. Williams 1987, *Journal of Physics E: Sci. Inst.* **20**, 1411
- [10] R. Felici, J. Penfold, R. C. Ward and W. Williams 1988, *Applied Physics A: Solids and Surfactants*, **45**, 169
- [11] D. G. Bucknall, J. Penfold, J. R. P. Webster, A. Zerbakhsh, R. M. Richardson, A. Rennie, J. S. Higgins, R. A. L. Jones, R. K. Tomas, S. Roser and E. Dickinson 1995, "SURF - a second generation neutron reflectometer," in *Proceedings of the meetings ICANS-XIII and ESS-PM4*, Villigen
- [12] D. Keen 2007, "LMX - A diffractometer for large molecular crystallography draft proposal,"
- [13] R. I. Bewley, J. W. Taylor and S. M. Bennington 2011, "LET, a cold neutron multi-disk chopper spectrometer at ISIS," *Nucl. Instr. Meth. Phys. Res. A*, **637**, 128-134
- [14] Applied Scintillation Technologies Ltd, [Online]. Available: <http://www.appscintech.com/>.
- [15] G. J. Sykora, E. M. Schooneveld, N. J. Rhodes and L. Van Eijck 2012, "Gamma Sensitivity of a ZnS:Ag(6-LiF) Wavelength Shifting Fibre Detector in Mixed Neutron-gamma Fields," in *IEEE Nuclear Science Symposium and Medical Imaging*,